J.Natn.Sci.Foundation Sri Lanka 2022 50 (4): 785 - 798
DOI: http://dx.doi.org/10.4038/jnsfsr.v50i4.10902

RESEARCH ARTICLE

Polymer science and technology

# Synthesis of polyethylene glycol-grafted graphite and effect of its loading on properties of natural rubber composites

**WDM Sampath[1,2*], CAN Fernando[1] and DG Edirisinghe [2]**
[1] *Department of Nano Science Technology, Faculty of Technology, Wayamba University of Sri Lanka, Kuliyapitiya 60200, Sri Lanka.*
[2] *Rubber Technology and Development Department, Rubber Research Institute of Sri Lanka, Telawala Road, Ratmalana 10390, Sri Lanka.*

Submitted: 24 January 2022; Revised: 01 June 2022; Accepted: 24 June 2022

**Abstract:** Modified graphite has attracted considerable interest over recent years due to its surface functionality and better dispersibility with polymeric materials. Incorporation of a small quantity of modified graphite filler into polymer can create novel composites with improved properties. In this study, polyethylene glycol (PEG) was grafted onto the graphite surface in the presence of maleic anhydride (MAH). The PEG-grafted graphite (PEG-g-Graphite) was characterized via Fourier Transform infrared spectroscopy (FTIR), X-ray diffraction spectroscopy (XRD), thermogravimetric analysis (TGA), and scanning electron microscopy (SEM), and the analysis proved that PEG was successfully grafted onto the graphite surface. Subsequently, natural rubber (NR) composites were prepared by varying the PEG-g-Graphite loading from 0 phr (parts per hundred rubber) to 10 phr at 2 phr intervals. The 10 phr PEG-g-Graphite filled NR composite showed an increment in scorch time and cure time in comparison to the NR composite prepared without PEG-g-Graphite (control). Further, heat resistance of the PEG-g-Graphite/NR composites prepared with 8 and 10 phr loadings of PEG-g-Graphite was at a high level. Due to sheet resistance, values of the 10 phr loading of PEG-g-Graphite and the control composites were $2 \times 10^5$ and $3.9 \times 10^7$ ohms/square, respectively. The NR composite prepared with 10 phr loading of PEG-g-Graphite could be suitable for high electrical conductive polymeric applications.

**Keywords**: Graphite, natural rubber composites, polyethylene glycol, polyethylene glycol-grafted graphite.

## INTRODUCTION

Graphite is a well-known filler material used in the rubber industry, and it is a naturally abundant, relatively low cost, and lightweight material when compared to other carbon allotropes (Mokhena *et al*., 2018). It is reported as the best conductive filler for its excellent conductive properties. Additionally, it has good mechanical properties and disperses well in a polymer matrix (Rus *et al*., 2016). Polymer/graphite composites are widely used for different applications such as sensors, memory material, and energy storage, due to their excellent electrical and thermal conductivity (Zhao *et al*., 2015). Polymer/graphite composites have been used in many applications including structural and aerospace materials, and sporting goods (Mokhena *et al*., 2018). A study conducted by Shih *et al*. (2010) revealed that graphite incorporated with polydimethylsiloxane (PDMS) shows the highest temperature sensitivity and higher thermal stability than the composites containing conventional carbon-based fillers. Moreover, graphite has been incorporated to polyurethane, silicone rubber, and epoxy resins to prepare composite materials to be used in the preparation of electrodes for different industrial applications (Calixto *et al*., 2007). A composite prepared with polypropylene (PP) and graphite showed a significant improvement

* Corresponding author (wikcramage@yahoo.com; https://orcid.org/0000-0002-6481-7189)

of the surface tension with increasing graphite content, and the composite was applied to adhesives in fuel cell applications (Rzeczkowski *et al*., 2019).

Graphite consists of carbon atoms trigonally bound to each other by covalent bonds, forming hexagonal rings. Each carbon is $sp^2$-hybridized with three of the four valence electrons used to form bonds to each of the three attached carbon atoms (Mokhena *et al*., 2018; Sampath *et al*., 2021). The fourth electron resonates freely within the graphene layer, and generates van der Waals forces acting between adjacent graphene layers (Mokhena *et al.*, 2018). Several graphite modification methods have been carried out to improve its dispersion in different polymeric materials. In this study, graphite is modified by grafting polyethylene glycol (PEG) to enhance the performance of the final composite, and further it was noted that unmodified graphite disperses poorly in the polymer matrix. PEG is nontoxic, biocompatible, and heat resistant, and could be used as a dispersant and a toughening agent (Huang *et al*., 2019). The characteristic behaviour of PEG seems to be due to the crucial balance of the hydrophobic forces exerted by the ethylene units ($–CH_2–CH_2–$) with the hydrophilic interactions of the oxygen atoms present in the oxirane units and in the terminal groups (Zohuri, 2012). The thermal stability and processability of bamboo fibre (BF)/polylactic acid (PLA) composites have been developed with high molecular weight PEG (Long *et al*., 2019). Other than that, some polymer composites have been prepared by mixing different filler materials including metallic materials with graphite to generate different properties (Saraswati *et al*., 2020; Kitisavetjit *et al*., 2021).

Carbon nanotube (CNT) and graphite hybrid fillers have been used as reinforcing fillers in NR vulcanizates (Kitisavetjit *et al*., 2021) and the wettability of the CNT and graphite was assessed to elucidate filler dispersion in the NR matrix. NR composites prepared with 3 phr of CNT and 30 phr graphite have shown superior properties in terms of cure characteristics, mechanical properties and conductivity (Kitisavetjit *et al*., 2021). In another study, metal-graphene-filled hybrid polyamide composites have been developed and, combination of the two different fillers increased the mechanical properties up to 120% compared to the metal reinforced composites (Rad *et al*., 2019). In addition, the functionality of graphene (GNP) has been increased by grafting $NH_2$-poly(methyl methacrylate) (PMMA), and 2 wt. % of $NH_2$-PMMA-GNPs in PMMA were found to increase the elastic modulus, strength, and strain at break (Vallés *et al*., 2020).

Titanate base coupling agents have been utilized for modification of the graphite surface (Meng, 2012) and polymer composites have been prepared using capric acid (CA), myristic acid (MA) and poly-methyl methacrylate (PMMA) by varying titanate coated graphite powder loadings from 2–15% (w/w). The results indicated that the graphite/CA-MA/PMMA composites maintained good thermal storage performance, while the thermal expansibility became weaker (Meng, 2012). Most of the previous studies stated that graphite and modified graphite have been utilized to enhance the thermal and electrical performance of polymeric materials. No studies have been conducted regarding modified graphite incorporated NR composites and their performance. The main goal of this study is to enhance the physico-mechanical, thermal, electrical and rheological properties of NR composites using surface functionalized graphite obtained by grafting PEG on micro scale graphite powder.

## MATERIALS AND METHODS

### Materials

RSS-2 with a Plasticity Retention Index of 64 was supplied by the Rubber Research Institute of Sri Lanka. PEG with a number-average molecular weight of 4000 g $mol^{-1}$ was purchased from the local market. Maleic anhydride (MAH) was used as the grafting material and was obtained from Morex Lanka (Pvt.) Ltd., Sri Lanka. Graphite with a mean particle size of 14 micron was used as conductive filler and was obtained from Bogala Graphite Lanka Plc., Sri Lanka. N,N-dimethylformamide (DMF) and all rubber compounding ingredients were purchased from local suppliers.

### Synthesis of PEG-g-graphite

Figure 1 shows the fabrication procedure of PEG-g-Graphite. Graphite (5 g) was added to DMF (20 mL) to form a stable graphite / DMF suspension via ultrasonication (20kHz / 500W) for 30 min. The graphite / DMF mixture was then heated with an excess of MAH (10 g) at 100 ºC for 24 h under dry nitrogen. After the reaction, 10 g of PEG was added based on a 1:1 PEG: MAH ratio. The mixture was reacted at 80 ºC for 48 h through continuous mechanical stirring and poured into a beaker containing 98% ethanol. Then, the product obtained was filtered and washed several times to remove free PEG and MAH at low pressure. The final product was dried at 50 ºC in a vacuum oven (Huang *et al.*, 2019).

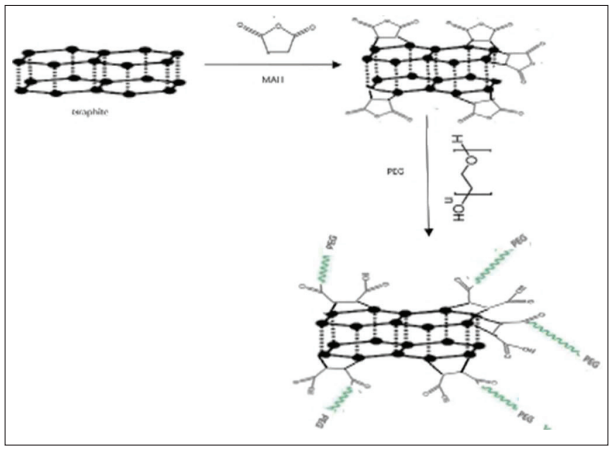


**Figure 1:** Schematic diagram of the PEG-g-graphite synthesis

## Preparation of PEG-g-Graphite/NR composites

A series of NR composites was formulated by varying the PEG-g-Graphite loading from 2 phr to 10 phr at 2 phr intervals. The NR composite prepared without PEG-g-Graphite was considered as the control. The formulation of the composites is given in Table 1.

**Table 1:** Formulation of the PEG-g-Graphite / NR composites

| Ingredient | Function | Phr |
|---|---|---|
| Natural rubber (RSS-2) | Rubber | 100 |
| ZnO | Inorganic activator | 5.0 |
| Stearic acid | Organic co-activator | 2.0 |
| TMQ | Antioxidant | 1.0 |
| PEG-g-Graphite | Conductive filler | 0,2,4,6,8,10 |
| ZDC | Accelerator | 1.5 |
| Sulphur | Vulcanizing agent | 2.0 |

**Table 2:** Mixing cycle of the PEG-g-Graphite/NR composites

| Total time, min | Ingredient |
|---|---|
| 0 | Added NR |
| 1 | Added Zinc oxide + Stearic acid + TMQ |
| 2 | Added PEG-g-Graphite |
| 5 | Added ZDC |
| 6 | Added Sulphur |
| 14 | Dumped the compound |

The composites were prepared by melt mixing using a Brabender Plasticorder operated at room temperature, at a rotor speed of 60 rpm. The total mixing time was kept constant at 10 min. The mixing cycle used in the preparation of NR composites is given in Table 2. The composites were compressed in an electrically heated hydraulic press machine at 150 °C under a pressure of 0.35 MPa to produce 2 mm thick sheets. Test specimens were cut from these sheets according to the required standards.

## Characterization

X-ray diffraction (XRD) analysis was conducted using an X-ray diffractometer (UltimaIV, Japan) to confirm the crystallographic nature of graphite and PEG-g-Graphite materials. The PEG-g-Graphite and graphite materials were scanned in continuous mode by varying the scanning angle from 0.50 to 90.0 degrees at a scanning speed of 3 degrees per minute in 2θ (degrees). Further, chemical structures of graphite and PEG-g-Graphite were characterized using a Nicolet 380 FTIR spectrometer. Spectra were recorded in the range of 400 –3500 $cm^{-1}$ operated at 4 $cm^{-1}$ resolution. The surface morphology of graphite, PEG-g-Graphite and tensile fracture surfaces of PEG-g-Graphite/NR composites were examined by Scanning Electron microscopy (SEM) using a ZEISS EVO LS 15 Microscope. The specimens were sputter coated with a thin layer of gold to avoid electrostatic charging during examination. The thermal stability of the two materials was investigated through thermogravimetric analysis (TGA) (TGA 400, Perkin Elmer) at a heating rate of 10 ºC / min from room temperature to 600°C in a nitrogen atmosphere.

### *Cure characteristics*

Cure characteristics of PEG-g-Graphite/NR composites, such as minimum torque (ML), maximum torque (MH), scorch time ($Ts_2$), optimum cure time ($T_{90}$), cure rate index (CRI), and extent of cure or delta cure (MH-ML), were obtained by a Dynamic Rubber Process Analyzer (D-RPA 3000- MonTech, Germany) at 150 ºC.

### *Physico-mechanical properties*

Tensile properties and tear strength of PEG-g-Graphite/NR composites were determined using Instron tensile testing machine according to BS ISO 37:2017 and BS ISO 34-1:2015, respectively. Dumb-bell shaped tensile test specimens and angle shaped tear test specimens were used. The cross-head speed was maintained at 500 mm/min. The hardness of the composites was

determined using Digi Test hardness tester according to BS ISO 48-4:2018. The resilience of the composites was measured by a Wallace Lupke pendulum in accordance with ISO 4662: 2017.

### *Ageing properties*

Accelerated ageing of the composites was carried out at 70 ºC for 72 hours in an air circulating oven. Tensile properties were evaluated after ageing, and percentage retention of these properties was calculated according to equation 1.

$$\text{Retention of tensile strength (\%)} = \frac{\text{Tensile strength after ageing}}{\text{Tensile strength before ageing}} \times 100 \quad \ldots(1)$$

### *Sheet resistance*

Sheet resistance of PEG-g-Graphite/NR composites was assessed using a four-probe electrical conductivity meter (Jandel RM 3000). The specimens were cut into 10 mm × 10 mm square-shaped pieces of 1 mm thickness.

## RESULTS AND DISCUSSION

### Characterization of graphite and PEG-g-Graphite

Figure 2 shows the comparison of FTIR spectra between graphite and PEG-g-Graphite. After the MAH and PEG reaction, a wide broad peak has appeared at 3340 $cm^{-1}$ corresponding to the stretching vibration of O-H groups (Rawn & Ouellette, 2018). Further, asymmetrical and symmetrical stretching vibrations of C-H bonds are assigned at 2935 and 2915 $cm^{-1}$; these belong to the PEG molecular chain (Huang *et al*., 2019). In addition, the narrow peak at 1028 $cm^{-1}$ is attributed to the stretching vibration of C-O-C bond in the ester groups of PEG-g-Graphite owing to the reaction of the hydroxyl group with MAH (Xu *et al.*, 2015). Hence, FTIR results suggest that PEG molecules are chemically grafted to the graphite through the esterification reaction with the MAH coupling agent.

XRD patterns of graphite and PEG-g-Graphite are shown in Figure 3. Graphite powder shows a characteristic peak at 2θ = 26.6º (Volanti *et al*., 2015). When PEG is grafted to graphite, the graphitic peak shifts to 2θ = 26.73º. In addition, two extra narrow peaks have appeared at 2θ = 23.65º and 2θ = 31.36º due to grafting PEG via the MAH (Barron *et al*., 2003). In addition, graphite shows two other very low peaks at 2θ = 44.65º and 2θ = 54.67º. However, these peaks are shifted to 2θ = 44.08º and 2θ = 54.54º, respectively due to incorporation of PEG.

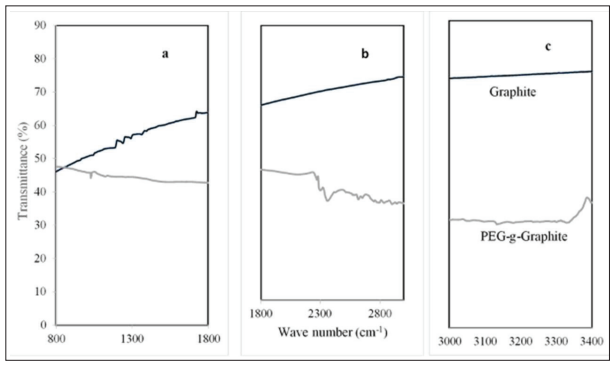


**Figure 2:** FTIR spectra of Graphite and PEG-g-Graphite for different regions\s
a) 800 to 1800 $cm^{-1}$; b) 2000 to 3000 $cm^{-1}$; c) 3000 to 3400 $cm^{-1}$

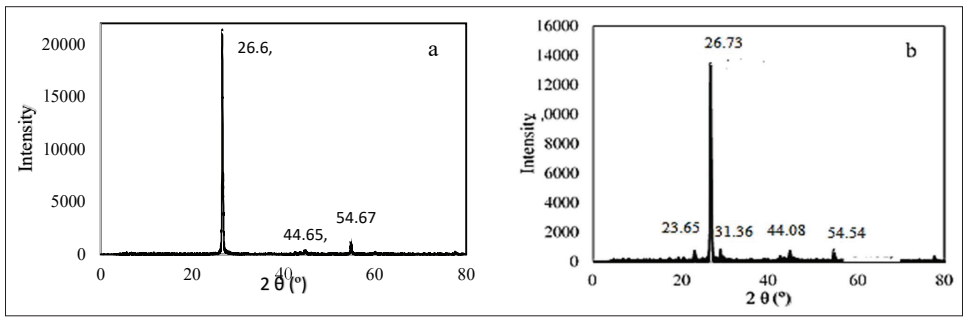


**Figure 3:** XRD diffractogram of (a) Graphite (b) PEG- g-Graphite

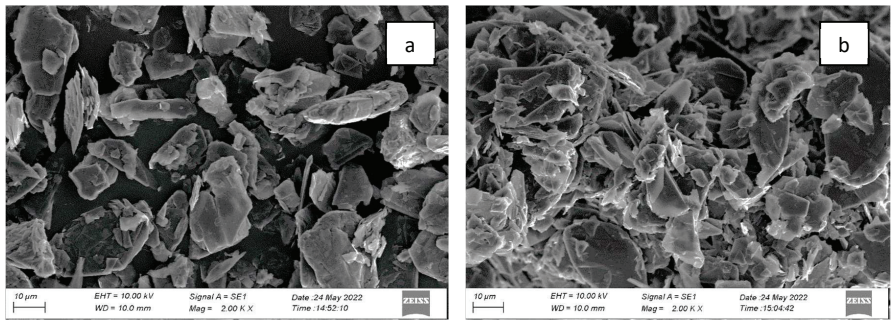


**Figure 4:** SEM images of surface of (a) graphite and (b) PEG-g-graphite

The surface morphologies of the graphite and PEG-g-Graphite were studied using SEM as shown in Figure 4. As seen in this figure, graphite [Figure 4(a)] looks like a thin "petal" flake with a typical lamella structure (Esmaeili *et al*., 2020) in which graphene layers are not distinguishable. Further, the graphite surface has not shown good adhesion among the graphite particles. However, in PEG-g-Graphite [Figure 4(b)], the dispersibility and homogeneity of the graphite surface have been improved. Furthermore, the free volume of the PEG-g-Graphite is less than that of the graphite due to improved surface adhesion among the graphite particles via the PEG.

The PEG-g-Graphite sample was assessed via TGA (Figure 5) for confirmation of success of grafting. Based on the results, graphite exhibited no significant weight loss up to 600 °C. However, two weight loss stages are observed in PEG-g-Graphite after its modification. The primary mass loss of the grafted samples is indicated in the temperature range 120 – 205 °C, which is assigned to the degradation of the moiety deriving from the grafted MAH molecules (Samadaei *et al*., 2016). The major weight loss of grafted sample occurs at the temperature range approximately between 205–400 °C, which originates from the grafted PEG chain (Kou *et al*., 2019).

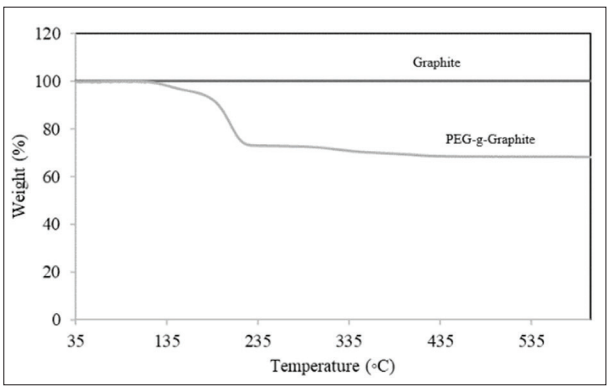


**Figure 5:** TGA curves of graphite and PEG-g-graphite

### *Cure characteristics of PEG-g-Graphite/ NR composites*

Minimum torque (ML) is an indication of stock viscosity and processability of rubber composites (Ismail *et al*., 2002). Maximum torque (MH) is an indication of the state of cure, whereas delta cure (MH-ML) is an indication of cross-link density of rubber composites (Surya *et al*., 2018). Table 3 shows that addition of 2 phr of PEG-g-Graphite has increased ML and MH of the composite in comparison to the control. Accordingly, delta cure has also increased with the addition of 2 phr of PEG-g-Graphite. All the composites prepared with PEG-g-Graphite show higher ML and MH than the control. Furthermore, when the PEG-g-Graphite loading is increased beyond 4 phr, ML of PEG-g-Graphite/NR composites has decreased, due to the effect of increased wettability and low density of graphite-based materials (Kitisavetjit *et al*., 2021). The addition of 2 phr PEG-g-Graphite has increased MH and (MH-ML) torque of the PEG-g-Graphite/NR composite in comparison to the control, while the literature indicates an improvement of reinforcing efficiency, crosslink density and better filler dispersion on NR matrix (Surya *et al*., 2018; Kitisavetjit *et al*., 2021).

In addition, the increase in the PEG-g-Graphite loading has increased scorch time and cure time of NR composites (Table 3). Scorch time, which indicates processing safety, ranges from 0.61 min to 0.83 min in the composites. The control composite has shown the

lowest scorch time and cure time due to poor viscosity of the material (Ismail *et al*., 2002). Further, it is reported in literature that the cross-link density and thermal conductivity of graphite filled rubber compounds increase with the increase of graphite percentage (Somaweera *et al*., 2021). However, composites prepared with PEG-g-Graphite have shown a low cure time at 150 ºC since graphite has a higher possibility to form agglomerates in the NR matrix at a low loading level (Sumita *et al*., 1991). Additionally, Matthew *et al*. (2019) found that PEG could act as an activator in NR composites. This could be another reason for the low values of scorch and cure times shown by all PEG-g-Graphite filled NR composites.

**Table 3:** Cure characteristics of PEG-g-Graphite/NR composites

| Property | PEG-g-graphite loading | | | | | |
|---|---|---|---|---|---|---|
| | 0 Phr | 2 Phr | 4 Phr | 6 Phr | 8 Phr | 10 Phr |
| Minimum torque, ML (dNm) | 0.39 | 0.66 | 0.66 | 0.56 | 0.43 | 0.61 |
| Maximum torque, MH (dNm) | 6.79 | 7.92 | 7.51 | 6.84 | 6.80 | 7.02 |
| Scorch time, $Ts_2$ (Min) | 0.61 | 0.71 | 0.74 | 0.81 | 0.83 | 0.81 |
| Cure time, $T_{90}$ (Min) | 1.55 | 1.63 | 1.61 | 1.66 | 1.67 | 1.77 |
| Cure rate index, CRI ($Min^{-1}$) | 106.3 | 108.6 | 114.9 | 117.6 | 119.0 | 104.2 |
| Delta cure ((MH-ML) torque) (dNm) | 6.60 | 7.26 | 6.85 | 6.28 | 6.35 | 6.41 |

The increase in cure time with the increase of filler loading, a known effect in rubber vulcanization due to restriction of cross-link formation, has been reported in the literature (Shanmugharaj *et al*., 2019). The composite prepared with 10 phr loading of PEG-g-Graphite showed about a 14% increase in cure time compared to the control. CRI indicates the rate of crosslink formation of a sample. An 8.5–12% increase in CRI has been observed for the composites prepared with 4-8 phr PEG-g-Graphite in comparison to the control, probably due to enhancement of filler-rubber interaction as reported in the literature (Sumita *et al*., 1991). However, 10 phr of PEG-g-Graphite filled composite exhibits a lower CRI than the control. This can be a result of the high increase in cure time shown by the 10 phr PEG-g-Graphite composite compared to the control (Hassan *et al*., 2012).

Moreover, cure characteristics depend upon filler properties such as the nature of the filler, surface area, surface reactivity, aspect ratio, and particle size (Shanmugharaj *et al.*, 2019). As stated earlier, graphite particles are chemically inert and do not react with the rubber matrix, and hence, air voids could be formed around the graphite particles (Shanmugharaj *et al*., 2019). This could be a reason for cure characteristics not showing a large variation with the increase of PEG-g-Graphite loading.

### *Physico-mechanical properties of PEG-g-Graphite/ NR composites*

Stress-strain curves provide an extremely important graphical measure of mechanical properties of a material such as modulus, tensile strength and elongation at break. These parameters are highly important to explain the elastic behaviour of a material. Figure 6 shows the stress-strain behaviour of NR composites with and without PEG-g-Graphite. The composite prepared with 10 phr loading of PEG-g-Graphite shows higher stress-strain properties compared to the other PEG-g-Graphite filled composites and the control. Generally, toughness of rubber composites increases with filler loading (Bokobza, 2017). Hence, 10 phr PEG-g-Graphite loaded composite shows the highest toughness, which is indicated by the highest area under the stress-strain curve. In addition, the area under this curve represents the elastic potential energy of a polymeric material (Sampath *et al*., 2019a; 2019b). Hence, the composite prepared with 10 phr loading of PEG-g-Graphite shows a higher elastic potential energy per unit volume ($4873.5 \times 10^6$ $Jm^{-3}$) than the other composites.

The variation of hardness of NR composites with PEG-g-Graphite loading is shown in Figure 7. The hardness of all six composites is observed in the range

40–45 IRHD. The hardness of all the composites prepared with PEG-g-Graphite is higher than that of the control. The hardness of a polymeric material is a measure of its stiffness (Edirisinghe & Freakley, 2003). The composite prepared with 10 phr loading of PEG-g-Graphite shows the highest hardness and this can be attributed to the highest toughness indicated earlier by the area under the stress-strain curve.

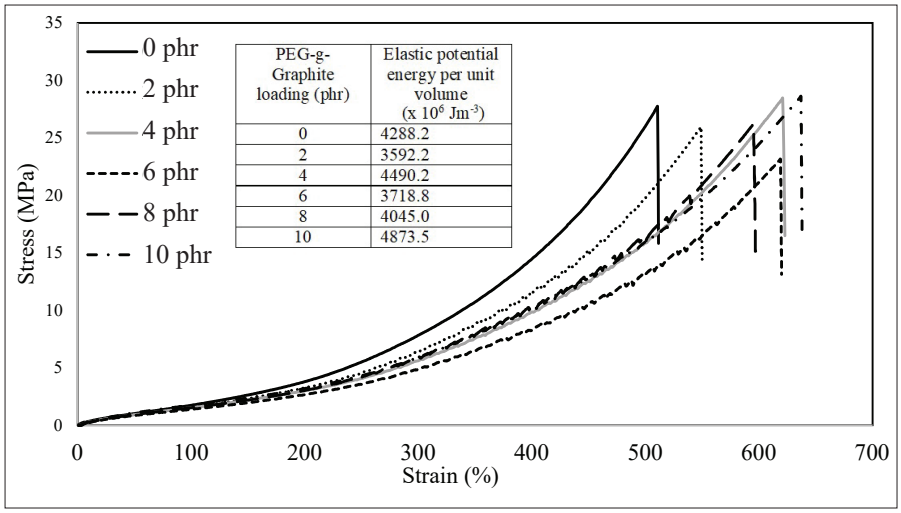


| PEG-g-Graphite loading (phr) | Elastic potential energy per unit volume (x $10^6$ $Jm^{-3}$) |
|---|---|
| 0 | 4288.2 |
| 2 | 3592.2 |
| 4 | 4490.2 |
| 6 | 3718.8 |
| 8 | 4045.0 |
| 10 | 4873.5 |

**Figure 6:** Stress-strain properties of PEG-g-Graphite/NR composites

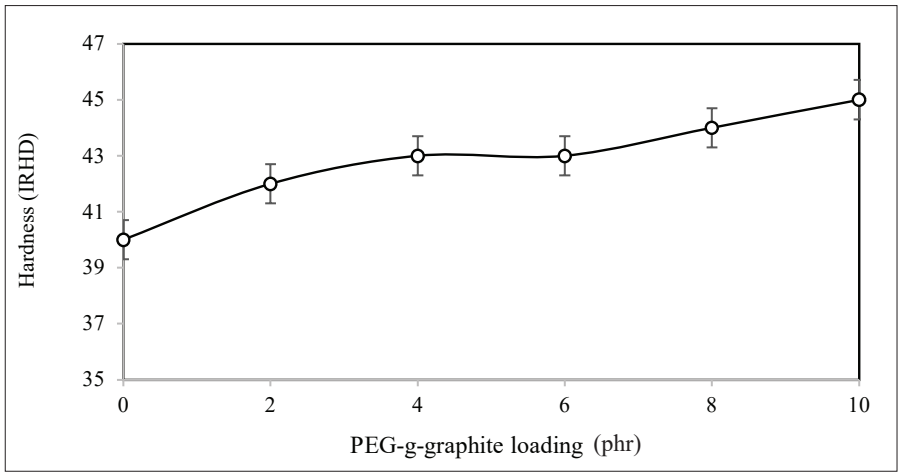


**Figure 7:** Hardness of PEG-g-Graphite / NR composites

Tensile strength and modulus at 300% elongation of the NR composites vary according to a cyclic pattern with the increase of PEG-g-Graphite loading, as shown in Figures 8 and 9, respectively. This behaviour can be attributed to the combined effect of the plasticizing action of graphite (Imiela *et al.*, 2019) and the agglomeration of graphite-based materials at low loading levels (Kitisavetjit *et al.*, 2021). The composite prepared with 2 phr loading of PEG-g-Graphite shows the highest modulus at 300% elongation, and this can be attributed to the highest crosslink density, as indicated by the (MH-ML) torque values (Table 3).

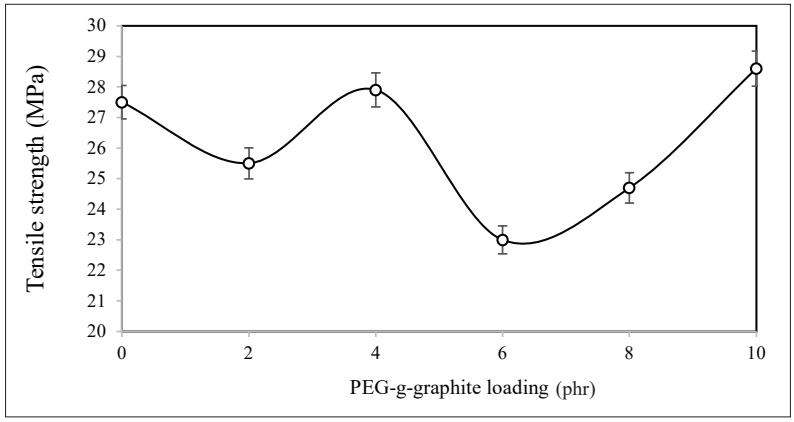


**Figure 8:** Tensile strength of PEG-g-Graphite / NR composites

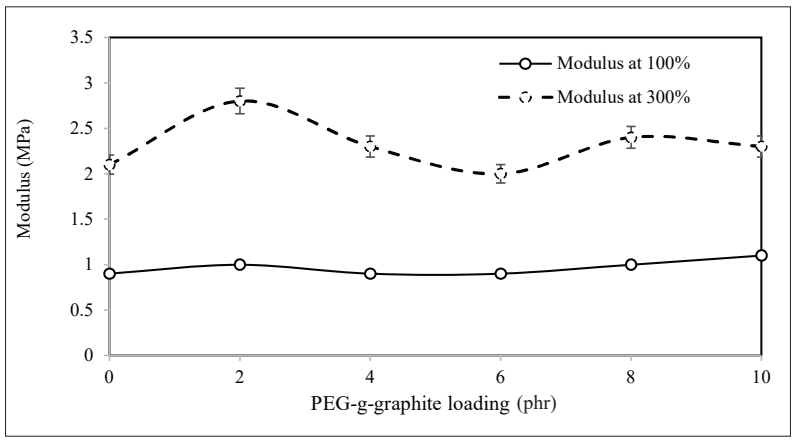


**Figure 9:** Modulus at 100% and 300% elongations of PEG-g-Graphite/NR composites

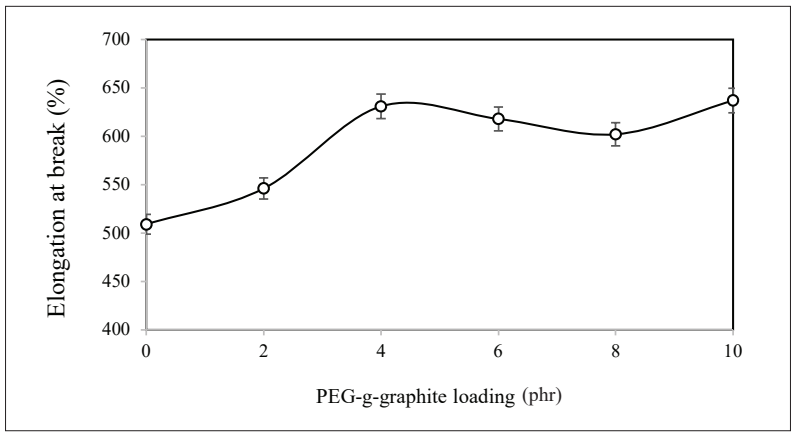


**Figure 10:** Elongation at break of PEG-g-Graphite/NR composites

All the composites exhibit similar tangents at 100% elongation (Figure 6) and hence modulus at 100% elongation of NR composites has not shown a significant variation with the increase of PEG-g-Graphite loading (Figure 9).

Elongation at break of the composites has also varied in a cyclic pattern with the increase of PEG-g-Graphite loading (Figure 10); however an increasing trend is observed. Elongation at break of PEG-g-Graphite based composites is higher than that of the control due to the presence of long–chain organic PEG molecules, which encourage compatibility with the NR matrix leading to improved dispersion (Maiti *et al*., 2017). In addition, PEG is a strong bio-compatible polymeric material (Huang *et al*., 2019) and hence forms chemical linkages between the NR phase and graphite surface effectively. The higher elongation at break shown by the NR composite prepared with 10 phr loading of PEG-g-Graphite compared to other NR composites indicates better adhesion between NR and PEG-g-Graphite material in the former composite. Huang *et al*. (2019) reported a similar observation in regard to elongation at break of PEG-g-Graphene filled poly (lactic acid) nanocomposites.

The resistance to initiate and propagate a crack is measured by tear strength. Similar to tensile strength, tear strength also varies according to a cyclic pattern with the increase of PEG-g-Graphite loading (Figure 11). Variation in tear strength could be considerably affected by the change from crystallinity in the morphology of the interface. The tear strength of most of the NR composites prepared with PEG-g-Graphite is higher than that of the control and may be due to existence of a strong interface between the NR matrix and PEG-g-Graphite due to improved adhesion between the two materials.

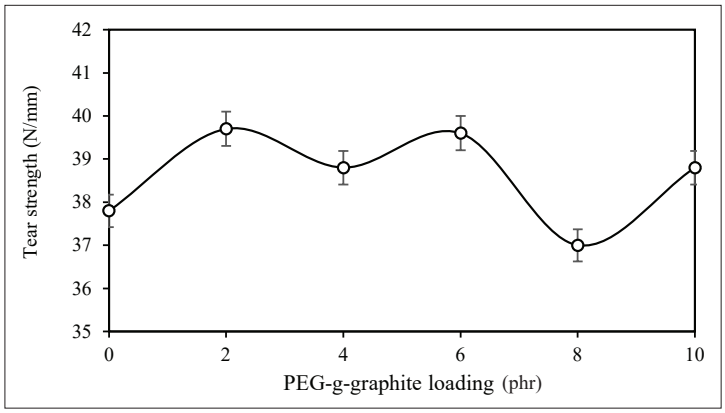


**Figure 11:** Tear strength of PEG-g-Graphite/NR composites

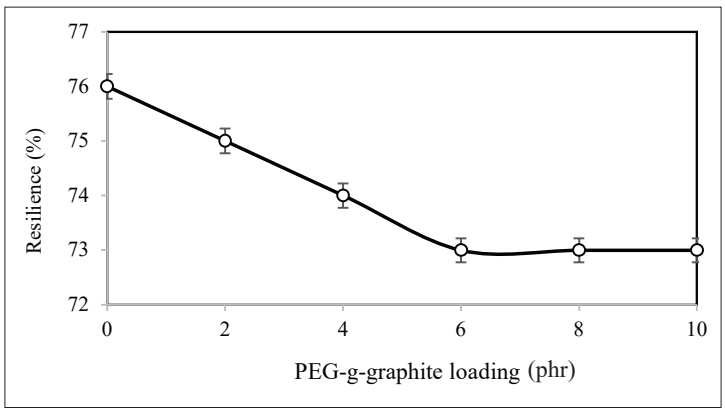


**Figure 12:** Resilience of PEG-g-Graphite / NR composites

The resilience of a polymeric material emphasizes the flexibility and elastic behaviour of a material. The control composite has indicated the highest resilience due to the absence of PEG-g-Graphite as the filler material (Figure 12). However, there is no marked difference in resilience between the PEG-g-Graphite composites and the control. Generally, resilience decreases with the increase in hardness and hence the resilience results are in agreement with the hardness results. Further, it can be stated that higher PEG-g-Graphite loadings in NR composites lead to an increase in the ability to transform mechanical energy into heat, thus decreasing the rebound resilience.

### *Tensile properties of PEG-g-Graphite / NR composites after ageing*

Table 4 shows the tensile properties, after ageing of the control, and the other NR composites prepared with different PEG-g-Graphite loadings. The composites prepared with PEG-g-Graphite loadings of 8 phr and 10 phr have shown higher retention of tensile properties, and hence exhibit higher resistance to thermal degradation. The control and NR composites prepared with PEG-g-Graphite loadings of 2 phr and 4 phr indicate poor resistance to thermal degradation. In other words, during ageing, low loadings of PEG-g-Graphite are not sufficient to retain the strong interactions formed with the NR matrix. In addition, PEG is a polymeric material with a low melting point and hence, low loadings of PEG-g-Graphite would not be sufficient to provide better adhesion between PEG and NR. A conventional sulphur vulcanizing system was used in this study. Matthews *et al*. (2019) reported that initial polysulphide crosslinks formed from the conventional sulphur vulcanizing system react further to form weak mono-, di-, and cyclic sulphide bonds during vulcanization via the dissociation, recombination, and rearrangement of the sulphur linkages. Therefore, the initial polysulphidic crosslinks formed are thermally unstable and hence undergo homolytic scission of the sulphur bonds and thermal decomposition and desulphuration, leading to weaker bonds. Deterioration of tensile properties of the NR composites observed with ageing at low loadings of PEG-g-Graphite is a result of the above-mentioned phenomena.

**Table 4:** Retention of tensile properties of PEG-g-Graphite / NR composites after ageing

| Property | PEG-g-Graphite loading (phr) | | | | | |
|---|---|---|---|---|---|---|
| | 0 | 2 | 4 | 6 | 8 | 10 |
| Retention of tensile strength (%) | 12.18 | 14.51 | 16.77 | 58.39 | 91.54 | 83.92 |
| Retention of elongation at break (%) | 57.37 | 52.21 | 55.47 | 76.54 | 87.71 | 86.97 |

**Table 5:** Sheet resistance of PEG-g-Graphite/NR composites

| Property | PEG-g-Graphite loading (phr) | | | | | |
|---|---|---|---|---|---|---|
| | 0 | 2 | 4 | 6 | 8 | 10 |
| Sheet resistance ($\times 10^5$) (ohms/square) | 3879.58 | 2.10 | 2.08 | 2.03 | 2.00 | 2.00 |

### *Sheet resistance of PEG-g-Graphite / NR composites*

Sheet resistance of PEG-g-Graphite filled NR composites varies from $3.88 \times 10^8$ to $2 \times 10^5$ ohms/ square as shown in Table 5. The sheet resistance of a material is directly proportional to its resistivity. The composites prepared with PEG-g-Graphite have shown lower sheet resistance than the control. Hence, PEG-g-Graphite composites exhibit better electrical conductivity. Further, the electrical conductivity of polymeric materials depends on many factors such as particle shape of filler, polymer–filler interaction, nature of particle–particle boundary and influence of preparation conditions on the volume

distribution of conductive particles (Wu & McLachlan, 1997; Gonon & Boudefel, 2006). Hence, it is evident that PEG forms a strong interaction between NR and graphite. In addition, sheet resistance of PEG-g-Graphite composites has not shown a significant variation as it varies from $2 \times 10^5$ only to $2.1 \times 10^5$ ohms/square. It is to be noted that the sheet resistance of 10 phr PEG-g-Graphite loaded NR composite has decreased by 99.9% from that of control. The interaction between PEG-g-Graphite and NR has produced a unique material with enhanced electrical properties. Moreover, with the increase in PEG-g-Graphite loading, electrical conductive networks gradually form and penetrate into the insulating NR matrix. The literature reports that MAH and PEG molecular chains occupy a certain space, allowing graphite to overcome its attraction and disperse well (Huang *et al*., 2019). Hence, electrical conductivity has slightly increased with the increase of PEG-g-Graphite loading.

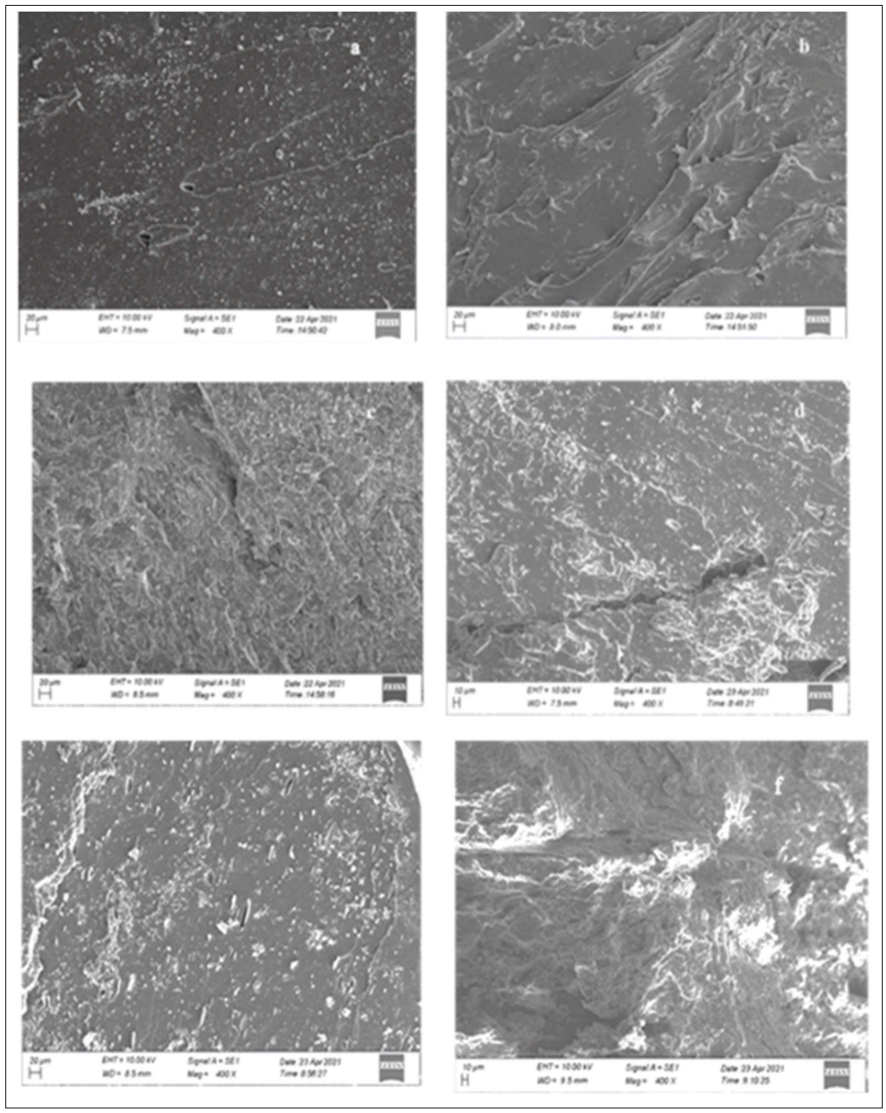


**Figure 13:** SEM images of tensile fracture surfaces of composites prepared with different PEG-g-Graphite loadings: (a) 0 phr (b) 2 phr (c) 4 phr (d) 6 phr (e) 8 phr and (f) 10 phr

### *Morphology of PEG-g-Graphite / NR composites*

The micrographs of the composites obtained via SEM are shown in Figure 13. As observed from Figure 13a, the fracture surface of the control (without PEG-g-Graphite) is smooth and planar. Further, it could be designated as a brittle fracture surface as it exhibits a low elongation at break according to Figure 10. On the other hand, the NR composites prepared with PEG-g-Graphite indicate an elastic nature, and also, this indication has been confirmed by the results of elongation at break of the composites. Furthermore, the NR composites prepared with 2, 4, and 6 phr loadings of PEG-g-Graphite have shown a weak interface of fracture surface and hence indicate poor surface adhesion [Figure 13(b-d)]. However, composites prepared with 8 and 10 phr loadings of PEG-g-Graphite show better surface adhesion [Figure 13(e-f)] as it homogenously disperses in the NR matrix and this has led to an improvement in properties.

## CONCLUSIONS

PEG-g-Graphite was synthesized successfully using MAH as coupling agent. Transformation of graphite to PEG-g-Graphite was confirmed by FTIR, XRD, and TGA techniques and SEM analysis. Scorch and cure times increased with the increase of PEG-g-Graphite loading. The 10 phr PEG-g-Graphite filled NR composite showed an increase in scorch time and cure time by 33% and 14%, respectively, in comparison to the NR composite prepared without PEG-g-Graphite (control). Also, the former composite (with10 phr PEG-g-Graphite) showed an enhancement in elongation at break and hardness compared to the latter composite (control). Ageing resistance of the PEG-g-Graphite/NR composites prepared with 8 and 10 phr loadings of PEG-g-Graphite was at a high level. Further, most of the physico-mechanical properties of PEG-g-Graphite/NR composites are at a level acceptable for super elastic rubber-based applications. The PEG-g-Graphite filled NR composites showed a remarkable improvement in electrical conductivity when compared to the control. The NR composite prepared with 10 phr loading of PEG-g-Graphite could be suitable for high electrical conductive polymeric applications.

**Acknowledgements**

The author wishes to thank the Rubber Research Institute of Sri Lanka, Bogala Graphite Lanka Plc. and Morex Lanka (Pvt.) Ltd., for supplying the raw materials for the study.

## REFERENCES

Barron M.K., Young T.J., Johnston K.P. & Williams R.O. (2003). Investigation of processing parameters of spray freezing into liquid to prepare polyethylene glycol polymeric particles for drug delivery. *Aaps Pharmscitech* **4**(2): 1–13. DOI: http://doi.org/10.1208/pt040212

Bokobza L. (2017). Mechanical and electrical properties of elastomer nanocomposites based on different carbon nanomaterials. *C-Journal of Carbon Research* **3**(2): 10. DOI: https://doi.org/10.3390/c3020010

Calixto C.M.F., Mendes R.K., Oliveira A.C.D., Ramos L.A., Cervini P. & Cavalheiro É.T.G. (2007). Development of graphite-polymer composites as electrode materials. *Materials Research* **10**: 109–114. DOI: https://doi.org/10.1590/S1516-14392007000200003

Edirisinghe D. & Freakley P.K. (2003). Effect of varied carbon black distribution on the morphology and properties of blends of natural and nitrile rubber. *Journal of the Rubber Research Institute of Sri Lanka* **86**: 58. DOI: https://doi.org/10.4038/jrrisl.v86i0.1807

Esmaeili Y., Zarrabi A., Mirahmadi-Zare S.Z. & Bidram E. (2020). Hierarchical multifunctional graphene oxide cancer nanotheranostics agent for synchronous switchable fluorescence imaging and chemical therapy. *Microchimica Acta* **187**(10): 1–15 DOI: https://doi.org/10.1007/s00604-020-04490-6

Gonon P. & Boudefel A. (2006). Electrical properties of epoxy/silver nanocomposites. *Journal of Applied Physics* **99**(2): 024308. DOI: https://doi.org/10.1063/1.2163978

Hassan H.H., Ateia E., Darwish N.A., Halim S.F. & Abd El-Aziz A.K. (2012). Effect of filler concentration on the physico-mechanical properties of super abrasion furnace black and silica loaded styrene butadiene rubber. *Materials and Design* **34**: 533–540. DOI: https://doi.org/10.1016/j.matdes.2011.05.005

Huang K., Yu H., Xie M., Liu S. & Wu F. (2019). Effects of poly (ethylene glycol)-grafted graphene on the electrical properties of poly (lactic acid) nanocomposites. *RSC Advances* **9**(19): 10599–10605. DOI: https://doi.org/10.1039/C9RA01060B

Ismail H., Nordin R. & Noor A.M. (2002). Cure characteristics, tensile properties and swelling behaviour of recycled rubber powder-filled natural rubber compounds. *Polymer Testing* **21**(5): 565–569. DOI: https://doi.org/10.1016/S0142-9418(01)00125-8

Imiela M., Anyszka R., Bieliński D.M., Masłowski M., Pędzich Z., Ziąbka M., Rybiński P. & Syrek B. (2019). Effect of graphite and common rubber plasticizers on properties and performance of ceramizable styrene–butadiene rubber-based composites. *Journal of Thermal Analysis and Calorimetry* **138**(4): 2409–2417. DOI: https://doi.org/10.1007/s10973-019-08339-w

Kitisavetjit W., Nakaramontri Y., Pichaiyut S., Wisunthorn S., Nakason C. & Kiatkamjornwong S. (2021). Influences of carbon nanotubes and graphite hybrid filler on properties

of natural rubber nanocomposites. *Polymer Testing* **93**: 106981.
DOI: https://doi.org/10.1016/j.polymertesting.2020.106981

Kou Y., Wang S., Luo J., Sun K., Zhang J., Tan Z. & Shi Q. (2019). Thermal analysis and heat capacity study of polyethylene glycol (PEG) phase change materials for thermal energy storage applications. *The Journal of Chemical Thermodynamics* **128**: 259–274.
DOI: https://doi.org/10.1016/j.jct.2018.08.031

Lai W.C., Liau W.B. & Lin T.T. (2004). The effect of end groups of PEG on the crystallization behaviors of binary crystalline polymer blends PEG/PLLA. *Polymer* **45**(9): 3073–3080.
DOI: https://doi.org/10.1016/j.polymer.2004.03.003

Long H., Wu Z., Dong Q., Shen Y., Zhou W., Luo Y., Zhang C. & Dong X. (2019). Effect of polyethylene glycol on mechanical properties of bamboo fiber reinforced polylactic acid composites. *Journal of Applied Polymer Science* **136**(26): 47709.
DOI: https://doi.org/10.1002/app.47709

Maiti M., Basak G.C., Srivastava V.K. & Jasra R.V. (2017). Influence of synthesized nano-ZnO on cure and physico-mechanical properties of SBR/BR blends. *International Journal of Industrial Chemistry* **8**(3): 273–283.
DOI: https://doi.org/10.1007/s40090-016-0107-7

Matthew C., Emmanuel O. & Lawrence E. (2019). Effects of polyethylene glycol as alternative activator in a bamboo fibre filled natural rubber composite. *Global Scientific Journal* **7**(5): 296–310.

Meng D. (2012). Effects of modified graphite on thermal properties of modified graphite/CA-MA/PMMA composite for latent heat thermal energy storage. *Advanced Materials Research* **562**: 401–404.
DOI: https://doi.org/10.4028/www.scientific.net/AMR.562-564.401

Mokhena T.C., Mochane M.J., Sefadi J.S., Motloung S.V. & Andala D.M. (2018). Thermal conductivity of graphite-based polymer composites. In: *Impact of Thermal Conductivity on Energy Technologies* (ed. A. Shahzad), pp. 181. IntechOpen Limited, London, UK.
DOI: https://doi.org/10.5772/intechopen.75676

Rad S.D., Islam A. & Alnasser A. (2019). Development of metal-graphene-filled hybrid composites: Characterization of mechanical, thermal, and electrical properties. *Journal of Composite Materials* **53**(24): 3363–3376.
DOI: https://doi.org/10.1177/0021998318812928

Rawn J.D. & Ouellette R.J. (2018). *Organic Chemistry: Structure, Mechanism, Synthesis*. Academic Press, 2nd edition, pp. 1033. Elsevier Science, Netherlands.

Rus A.Z.M., Abdullah N.M. & Abdullah M.F.L. (2016). Mechanical behavior of ultra violet (UV) curable renewable polymer/graphite (PG). *Indian Journal of Science and Technology* **9**(48): 1–4.
DOI: https://doi.org/10.17485/ijst/2016/v9i48/102157

Rzeczkowski P., Krause B. & Pötschke P. (2019). Characterization of highly filled PP/graphite composites for adhesive joining in fuel cell applications. *Polymers* **11**(3): 462.
DOI: https://doi.org/10.3390/polym11030462

Samadaei F., Salami-Kalajahi M. & Roghani-Mamaqani H. (2016). Radical coupling of maleic anhydride onto graphite to fabricate oxidized graphene nanolayers. *Bulletin of Materials Science* **39**(1): 229–234.
DOI: https://doi.org/10.1007/s12034-015-1135-1

Sampath W.D.M., Egodage S.M. & Edirisinghe D.G. (2019a). Effect of an organotitanate coupling agent on properties of calcium carbonate filled low-density polyethylene and natural rubber composites. *Journal of the National Science Foundation of Sri Lanka* **47**(1): 17–27.
DOI: http://doi.org/10.4038/jnsfsr.v47i1.8923

Sampath W.D.M., Egodage S.M. & Edirisinghe D.G. (2019b). Effect of peroxide loading on properties of natural rubber and low-density polyethylene composites. *Journal of Physical Science* **30**(3).
DOI: https://doi.org/10.21315/jps2019.30.3.4

Sampath W.D.M., Fernando C.A.N. & Edirisinghe D.G. (2021). Review on carbon black and graphite derivatives-based natural rubber composites. *Advances in Technology* **1**(1): 101–126.
DOI: https://doi.org/10.31357/ait.v1i1.4857

Saraswati T.E., Maharani D. & Widiyandari H. (2020). Copper oxide-based carbonaceous nanocomposites: Electrochemical synthesis and characterization. *AIP Conference Proceedings* **2243**(1): 020024.
DOI: https://doi.org/10.1063/5.0001626

Shih W.P., Tsao L.C., Lee C.W., Cheng M.Y., Chang C., Yang Y.J. & Fan K.C. (2010). Flexible temperature sensor array based on a graphite-polydimethylsiloxane composite. *Sensors* **10**(4): 3597–3610.
DOI: https://doi.org/10.3390/s100403597

Shanmugharaj A.M., Kumar K.T., Sundari G.S., Kumar E.S., Ashwini A., Ramya M., Varsha P., Kalaivani R., Raghu S. & Ryu S.H. (2019). Study on the effect of silica-graphite filler on the rheometric, mechanical, and abrasion loss properties of styrene–butadiene rubber vulcanizates. *Journal of Elastomers and Plastics* **51**(4): 359–378.
DOI: https://doi.org/10.1177/0095244318787560

Somaweera D., Abeygunawardane G.A., Weragoda S. & Ranatunga S. (2021). Effect of vein graphite powder on mechanical, curing, and thermal properties of solid tire vulcanizate. *Materials Today: Proceedings* **59**: 316–323.
DOI: https://doi.org/10.1016/j.matpr.2021.11.181

Sumita M., Sakata K., Asai S., Miyasaka K. & Nakagawa H. (1991). Dispersion of fillers and the electrical conductivity of polymer blends filled with carbon black. *Polymer Bulletin* **25**(2): 265–271.
DOI: https://doi.org/10.1007/BF00310802

Surya I., Hayeemasae N. & Ginting M. (2018). Cure characteristics, crosslink density and degree of filler dispersion of kaolin-filled natural rubber compounds in the presence of alkanolamide. *IOP Conference Series. Materials Science and Engineering* **343**(1): 012009.
DOI: https://doi.org/10.1088/1757-899X/343/1/012009

Vallés C., Papageorgiou D.G., Lin F., Li Z., Spencer B.F., Young R.J. & Kinloch I.A. (2020). PMMA-grafted graphene nanoplatelets to reinforce the mechanical and thermal properties of PMMA composites. *Carbon* **157**: 750–760. DOI: https://doi.org/10.1016/j.carbon.2019.10.075

Volanti D.P., Felix A.A., Suman P.H., Longo E., Varela J.A. & Orlandi M.O. (2015). Monitoring a CuO gas sensor at work: an advanced in situ X-ray absorption spectroscopy study. *Physical Chemistry Chemical Physics* **17**(28): 18761–18767. DOI: https://doi.org/10.1039/c5cp02150b

Wu J. & McLachlan D.S. (1997). Percolation exponents and thresholds obtained from the nearly ideal continuum percolation system graphite-boron nitride. *Physical Review B* **56**(3): 1236. DOI: https://doi.org/10.1103/PhysRevB.56.1236

Xu J.Z., Zhang Z.J., Xu H., Chen J.B., Ran R. & Li Z.M. (2015). Highly enhanced crystallization kinetics of poly (l-lactic acid) by poly (ethylene glycol) grafted graphene oxide simultaneously as heterogeneous nucleation agent and chain mobility promoter. *Macromolecules* **48**(14): 4891–4900. DOI: https://doi.org/10.1021/acs.macromol.5b00462

Zhao L.M., Feng X., Mi X.J., Li Y.F., Xie H.F. & Yin X.Q. (2015). Mechanical reinforcement and shape memory effect of graphite nanoplatelet-reinforced epoxy composites. *Journal of Intelligent Material Systems and Structures* **26**(12): 1491–1497. DOI: https://doi.org/10.1177/1045389X14544142

Zohuri G. (2012). *Polymer Science: A Comprehensive Reference*, 1st edition, pp. 7760. Elsevier Science, Netherlands.